

# Experimental study of heavy flavour production at HERA

*S. Boutle<sup>a</sup>, J. Bracinik<sup>b</sup>, A. Geiser<sup>c</sup>, G. Grindhammer<sup>d</sup>, A.W. Jung<sup>e</sup>, P. Roloff<sup>c,f</sup>, Z. Ruriková<sup>c</sup>, M. Turcato<sup>f</sup>, A. Yagües-Molina<sup>c</sup>*

<sup>a</sup> University College London, Gower Street, London WC1E 6BT, United Kingdom

<sup>b</sup> School of Physics and Astronomy, University of Birmingham - UK

<sup>c</sup> Deutsches Elektronen-Synchrotron DESY, Notkestraße 85, 22607 Hamburg, Germany

<sup>d</sup> Max-Planck-Institut f. Physik, Werner-Heisenberg-Institut Muenchen, Germany

<sup>e</sup> University of Heidelberg - Kirchhoff-Institute for Physics, Im Neuenheimer Feld 227, 69120 Heidelberg, Germany

<sup>f</sup> Universität Hamburg, Institut für Experimentalphysik, Luruper Chaussee 149, 22761 Hamburg, Germany

## Abstract

Recent measurements of charm and beauty production in  $ep$  collisions at HERA are reviewed. Heavy quark tagging methods used by the ZEUS and H1 experiments are described. Cross section results in both photoproduction and deep inelastic scattering (DIS) are compared with NLO QCD predictions. In general the data are well described by the calculations. Studies of charm fragmentation yield compatibility with the assumption of universality at large transverse momenta, but illustrate some problems with this assumption in the threshold region. The DIS cross sections can also be expressed in terms of the charm and beauty content of the proton,  $F_2^{c\bar{c}}$  and  $F_2^{b\bar{b}}$ . The most recent measurements are compared to next-to-leading order QCD predictions using different parameterisations of the theory, and of the gluon density in the proton. The tests of the fragmentation function, the gluon density, and details of the theoretical treatment of the charm and beauty masses are of direct interest to corresponding applications at the LHC.

*Coordinator/editor: A. Geiser*

## 1 Charm production at HERA: Experimental overview

*Author: A. Jung*

### 1.1 Introduction

Several new measurements of open charm production have been performed by the H1 collaboration

- $D^{*\pm}$  Production at low  $Q^2$  with the H1 Detector [1,2]
- Measurement of the  $D^{*\pm}$  Production cross section in Photoproduction with the H1 Detector using HERA II data [3]
- Study of Charm Fragmentation into  $D^{*\pm}$  Mesons in Deep-Inelastic Scattering at HERA [4]

and by the ZEUS collaboration

- $D^{*\pm}$  in DIS and Measurement of  $F_2^c$  [5]
- Measurement of  $D^{*\pm}$  Meson Production in DIS ep Scattering at low  $Q^2$  [6]
- Measurement of excited charm and charm-strange mesons production at HERA [7]
- Measurement of the charm fragmentation fractions [8] and fragmentation function [9]

The details of the measurements like the visible range will not be discussed here as they are given in the literature cited for each measurement. For both experiments high statistic charm event samples are tagged by  $D^{*\pm}$  mesons reconstructed in the golden decay channel:  $D^{*\pm} \rightarrow D^0 \pi_{\text{slow}}^\pm \rightarrow K^\mp \pi^\pm \pi_{\text{slow}}^\pm$ . The well known mass difference method reduces symmetric systematic uncertainties and allows the extraction of the  $D^*$  meson signal by fits out of the background dominated data samples. Other D mesons can also be identified via their characteristic mass peaks. In addition to that method charmed mesons like  $D^+$ ,  $D_s^+$  mesons are tagged via lifetime measurements from the high resolution silicon vertex detectors used by both experiments in HERAII.

The results on the fragmentation function will be discussed in section 2.

## 1.2 Results of open charm production

The H1 photoproduction analysis [3] makes use of the H1 Fast Track Trigger (FTT) [10, 11] which enhanced the capabilities of heavy flavor measurements at H1 by a selective on-line track based event reconstruction [12]. Due to these improvements the phase space and the available statistics of the measurement has been significantly enlarged compared to the previous H1 photoproduction analysis [13].

The large statistics allows precise double differential measurements. For the H1 photoproduction measurement the data are reasonably well described except for special regions of the phase space and correlations. Especially the  $W_{\gamma P}$  dependence is not described by the NLO prediction using the FFNS. The correlation between  $\eta$  and  $p_T$  as shown in Figure 1 (right) is compared to the NLO QCD predictions in the FFNS [14] and GM-VFNS; it turns out that the NLO QCD predictions are able to describe the correlation between  $\eta$  and  $p_T$  in photoproduction. Nevertheless the NLO predictions show an increasing deficit at forward  $\eta > 0$  which is largest at high  $p_T$  where the  $D^*$  data prefer the upper edge of the error band. For the photoproduction regime the relatively large theoretical uncertainty especially at small  $p_T$  arises from the scale variation. For comparison also the double differential measurement in DIS from H1 is shown on the left side of Figure 1. The H1 DIS analysis [1] uses the full HERAII luminosity. Because of the large statistics the analysis is almost everywhere dominated by the systematic error. The use of electron and hadron quantities combined in the  $e\Sigma$  reconstruction method [15] for the reconstruction of the kinematic variables allows lower inelasticities and smaller systematic uncertainties compared to previous H1 DIS analyses [2].

The measured single and double differential  $D^*$  production cross sections are in general well described by the next-to-leading order QCD predictions in the FFNS. The theoretical uncertainty of the predictions is dominated by the mass variation of the charm quark but is in general smaller than in photoproduction because of the additional scale  $Q^2$ . The small excess in data at forward directions  $\eta > 0$  (seen previously by H1 [2]) turns out to be located at low  $p_T$  as it can be seen

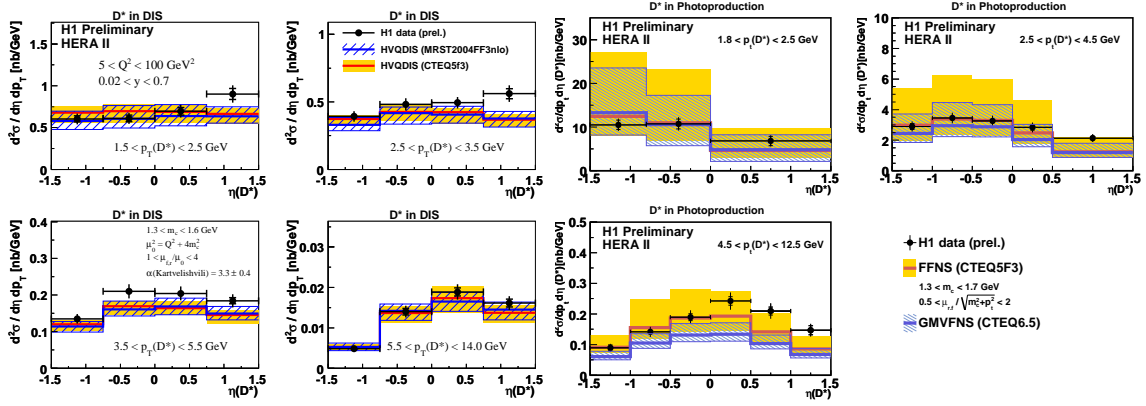


Fig. 1: The double differential cross section in  $\eta(D^*)$  and  $p_T(D^*)$  for the DIS (left) and photoproduction (right) regime compared to the NLO QCD predictions.

in comparison to the NLO prediction for the double differential distribution (see Figure 1 left). The data are above the predictions for the low  $p_T$  region at forward directions which is different to the photoproduction region where the data prefer the upper edge of the prediction at large  $p_T$ . The small discrepancy at forward directions can already be seen in the single differential  $\eta(D^*)$  distribution in comparison to the NLO QCD prediction as shown in Figure 2 left. The recent

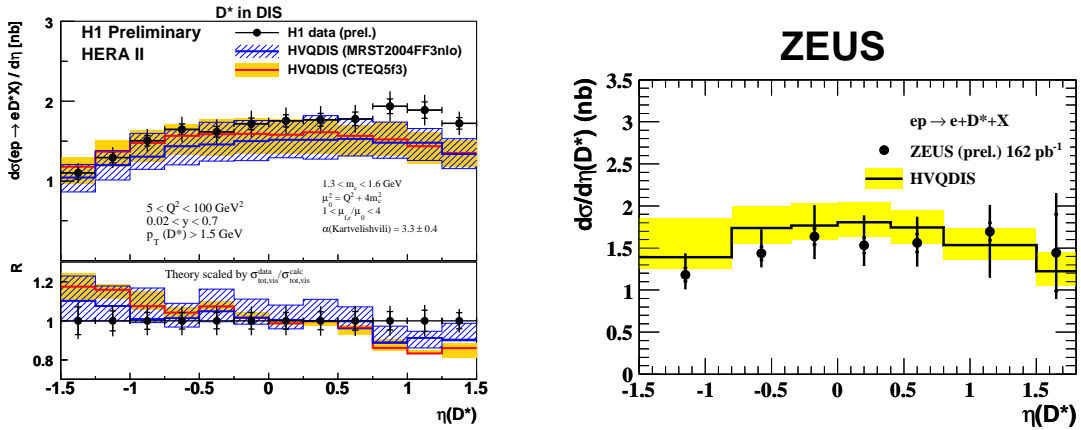


Fig. 2: The  $D^*$  cross section as a function of  $\eta(D^*)$  as measured by H1 using the luminosity of the whole HERAII data taking (left) and from ZEUS as measured using the luminosity of the years 2003 – 2005 (right).

$D^*$  measurement from the ZEUS collaboration [5] measures the same  $p_T(D^*)$  and  $y$  region but covers a slightly larger range in  $\eta(D^*)$  and goes up to larger  $Q^2$ . The ZEUS result (figure 2 right) is in good agreement with the NLO QCD predictions and in agreement with the result from H1 within errors.

A cross section measurement at very low  $Q^2$  for  $D^*$  production in DIS has been performed by ZEUS [6] using the beam pipe calorimeter. The overall  $Q^2$  range including this new measurement is shown in figure 3 (left) with a nice agreement to the NLO QCD prediction.

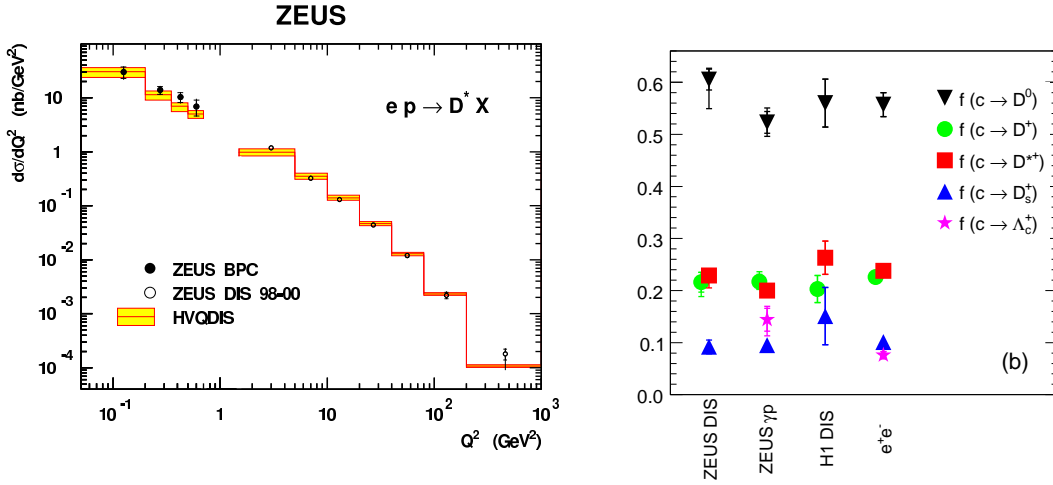


Fig. 3: The  $Q^2$  distribution including the new ZEUS measurement at very low  $Q^2$  shown right and the fragmentation fractions as measured by ZEUS and other experiment for various D mesons.

ZEUS has measured the charm production cross section of  $D^*$ ,  $D^0$ ,  $D^+$ ,  $D_s^+$  [8]. in order to determine the fragmentation fractions of charm into each meson. The charm fragmentation fractions as shown in figure 3 agree with the ones extracted by H1. Because of the agreement with the fragmentation fractions from  $e^+e^-$  the conclusion is that they do not depend on the hard subprocess and are in that sense universal.

In addition to the test of the QCD predictions in differential distributions another stringent test of QCD is possible since the  $D^*$  measurement involves the gluon density which drives the  $D^*$  production via the BGF production mechanism. Several approaches exist to measure the gluon density. The well established approach to measure the charm structure function will be covered elsewhere. In order to have an impact on the fits of the gluon density it is necessary that the cross section data have the highest possible precision. At present stage H1 and ZEUS enter the precision era of charm measurements where a single differential distribution has at least some sensitivity to the proton PDF, e.g. the  $\eta(D^*)$  distribution measured by H1 shows a better compatibility to the predictions if a proton PDF is used where a gluon density providing a less steep rise towards small  $x$  is used. However, the significance of the sensitivity is diminished by the relatively large theoretical uncertainties. The available  $D^*$  cross section data can also be used to fit the gluon density directly from the differential distributions in  $\eta(D^*)$ ,  $p_T(D^*)$ ,  $z(D^*)$ ,  $x$ ,  $Q^2$  [16].

In order to further increase the data precision it is possible to combine data from H1 and ZEUS on the basis of  $(D^*)$  cross sections or at the level of  $F_2^c$  extractions. At the level of  $F_2^c$  also the combination of data within one experiment from different  $F_2^c$  measurement methods, i.e. from  $D^*$  cross sections and from lifetime measurements, provides additional information.

### 1.3 Conclusions

At the present stage H1 and ZEUS enter the precision era of charm measurements with the large statistic of about  $0.5 \text{ fb}^{-1}$  per experiment provided by the HERAII running period. These data are currently analyzed and first preliminary results with high precision are available. In general the description by the next-to-leading order QCD predictions is reasonable except for some regions of the phase space. In order to get more insights and to have a significant impact on the fits of the PDFs the cross section data must be very precise and in addition cover the largest possible phase space. New results with such improvements are still expected to come.

## 2 Study of Charm Quark Fragmentation at HERA

*Authors: J. Bracinik, G. Grindhammer, Z. Rurikova*

The inclusive cross section for the production of heavy hadrons in  $ep$  collisions can be expressed as a convolution of three terms, describing the structure of the proton, the hard subprocess and the transition of partons to colourless heavy and light hadrons. The term describing the transition of partons to hadrons, also referred to as fragmentation function (FF), contains a non-perturbative component and thus must be experimentally determined. Charm quark fragmentation has been already extensively studied in  $e^+e^-$  annihilation experiments, and the parameters of various phenomenological models (i.e. the Lund string model, independent fragmentation model), which have been developed to describe the fragmentation process, have been tuned. By studying the charm quark fragmentation function also in  $ep$  collisions one can experimentally test, if the assumed universality of fragmentation functions, i.e. their portability from the calculation of processes in  $e^+e^-$  to processes in  $ep$  or  $pp/\bar{p}$ , really holds.

Since fragmentation functions describe the longitudinal momentum fraction transferred from the parton to the hadron they cannot be measured directly. The differential cross section as a function of suitably defined observables sensitive to the FF has to be measured and used to extract the parameters of the FF by comparing the data with the prediction of a given model.

The fragmentation of charm quarks into  $D^{*\pm}$  mesons in  $ep$  collisions has been studied by the H1 [17] and ZEUS [18] collaborations in both deep-inelastic scattering (DIS) and photoproduction (PHP), respectively. A so called hemisphere and a jet observable have been used by H1 and a jet observable by ZEUS.

In case of the jet observable, the momentum of the charm quark is approximated by the momentum of the reconstructed jet, which includes a  $D^{*\pm}$  meson, leading to the definition of  $z_{\text{jet}} = (E + P_L)_{D^*} / (E + P)_{\text{jet}}$ , where the longitudinal momentum  $P_{LD^*}$  is defined with respect to the three-momentum of the jet.

In case of the hemisphere observable, the kinematics of charm production, known to proceed mainly via photon-gluon fusion, is taken into account. In the  $\gamma^*p$  rest-frame the charm and anti-charm quarks are moving in the direction of the virtual photon (see figure 4 left), hence, the contributions from initial state radiation and the proton remnant can be strongly suppressed by discarding all particles with momenta pointing to the proton direction. Furthermore, since the transverse momenta of the charm quarks are balanced in this frame, the remaining particles may be divided into two hemispheres, one containing the fragmentation products of the charm quark, and the other one those of the anti-charm quark (see figure 4 right). This division into hemi-

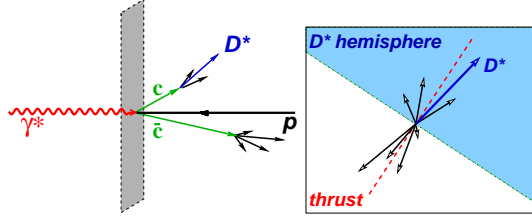


Fig. 4: Kinematics of charm/anticharm production in the  $\gamma^*p$  rest-frame as used for the definition of  $z_{hem}$ .

spheres is done by reconstructing the thrust axis in a plane perpendicular to the  $\gamma^*p$ -axis. The particles belonging to the same hemisphere as the  $D^{*\pm}$  meson are considered to be the products of the same quark and the sum of their four-momenta is used to approximate the four-momentum of the original quark, leading to this definition of  $z_{hem} = (E + P_L)_{D^*} / (E + P)_{hem}$ .

The ZEUS collaboration performed a measurement of the normalized differential cross section of  $D^{*\pm}$  meson production as a function of  $z_{jet}$  in photoproduction (kinematic range  $Q^2 < 1 \text{ GeV}^2$  and  $130 < W < 280 \text{ GeV}$ ). The  $D^{*\pm}$  mesons were reconstructed using the “golden” decay channel  $D^{*\pm} \rightarrow D^0 \pi_s^\pm \rightarrow K^\mp \pi^\pm \pi_s^\pm$ , requiring  $|\eta(D^{*\pm})| < 1.5$  and  $P_T(D^{*\pm}) > 2 \text{ GeV}$ . Jets were reconstructed using the inclusive  $k_\perp$  algorithm, requiring  $|\eta_{jet}| < 2.4$  and  $E_{T,jet} > 9 \text{ GeV}$ . Since the jets were reconstructed as massless, the jet observable reduces to  $z_{jet} = (E + P_L)_{D^*} / 2E_{jet}$ . The contribution of  $D^{*\pm}$  mesons from B-hadron decays, which amounts to about 9%, was subtracted using the prediction of the PYTHIA Monte Carlo program.

The H1 collaboration measured the normalized  $D^{*\pm}$  meson cross sections as a function of both  $z_{hem}$  and  $z_{jet}$  in DIS ( $2 < Q^2 < 100 \text{ GeV}^2$  and  $0.05 < y < 0.7$ ), using the same decay channel and requiring  $|\eta(D^{*\pm})| < 1.5$  and  $1.5 < P_T(D^{*\pm}) < 15 \text{ GeV}$ . Jets were reconstructed using the massive inclusive  $k_\perp$  algorithm in the  $\gamma^*p$  rest-frame. The measurement was performed for two event samples. In the first sample, referred to as the “ $D^{*\pm}$  jet sample”, the presence of a jet containing the  $D^{*\pm}$  with  $E_{T,jet} > 3 \text{ GeV}$  is required as a hard scale. In the second sample, the “no  $D^{*\pm}$  jet sample”, no such jet is present. The small 1 – 2% contribution of  $D^{*\pm}$  mesons originating from B-hadron decays was estimated with the RAPGAP MC and was subtracted from the data. Both measurements were corrected for detector and QED radiative effects.

The corrected data, shown in figure 5, were used to fit the parameters of fragmentation functions for two classes of QCD models: 1) the leading-order + parton shower models as implemented in the Monte Carlo programs RAPGAP (used by H1) and PYTHIA (used by ZEUS), interfaced with the Lund string model for fragmentation as implemented in PYTHIA, and 2) the next-to-leading-order (NLO) QCD calculations as implemented in HVQDIS (fixed flavor number scheme) and used by H1 for DIS, and in FMNR (variable flavor number scheme) used by ZEUS for photoproduction, with charm quarks fragmented independently to  $D^{*\pm}$  mesons. For comparison of the data with NLO calculations, hadronization corrections have been applied.

The values of the fragmentation function parameters  $\varepsilon$  and  $\alpha$  extracted for the Peterson and Kartvelishvili parametrizations respectively can be found in table 1. The optimal (at  $\chi_{min}^2$ ) fragmentation parameter value depends on the settings used for other free parameters of the PYTHIA model. With the default settings, the parameters extracted by ZEUS and H1 for the  $D^{*\pm}$  jet sam-

ple are in good agreement. When using the PYTHIA parameter settings tuned by ALEPH [19] a harder fragmentation function is needed to describe the data. This can be understood as being due to a significant fraction of  $D^{*\pm}$  mesons produced in decays of higher excited charm states, provided by the ALEPH setting in contrast to the default setting. The resulting value of the Peterson parameter, extracted by H1 using the  $D^{*\pm}$  jet event sample, is in agreement with the value  $\varepsilon = 0.040$  extracted by ALEPH from their data. This result is also consistent with the hypothesis of fragmentation universality in  $ep$  and  $e^+e^-$  processes.

For H1, in case of the HVQDIS NLO calculation, the data are well described after fitting the Kartvelishvili parametrization, while when using the Peterson one no satisfactory description of the data is achieved. In the case of ZEUS, both parametrizations are able to describe the data.

FF parametrization	ZEUS: PHP	H1: DIS		
		$D^{*\pm}$ jet sample		No $D^{*\pm}$ jet sample
	$z_{\text{jet}}$	$z_{\text{jet}}$	$z_{\text{hem}}$	$z_{\text{hem}}$
PYTHIA with default parameter setting:				
Peterson ( $\varepsilon$ )	$0.064 \pm 0.06^{+0.011}_{-0.008}$	$0.061^{+0.011}_{-0.009}$	$0.049^{+0.012}_{-0.010}$	$0.010^{+0.003}_{-0.002}$
Kartvelishvili ( $\alpha$ )	—	$3.1^{+0.3}_{-0.3}$	$3.3^{+0.4}_{-0.4}$	$7.6^{+1.3}_{-1.1}$
PYTHIA with ALEPH parameter setting [19]:				
Peterson ( $\varepsilon$ )	—	$0.035^{+0.007}_{-0.006}$	$0.029^{+0.007}_{-0.005}$	$0.006^{+0.002}_{-0.002}$
Kartvelishvili ( $\alpha$ )	—	$4.3^{+0.4}_{-0.4}$	$4.5^{+0.6}_{-0.5}$	$10.3^{+1.7}_{-1.6}$
NLO calculations FMNR (PHP) and HVQDIS (DIS):				
Peterson ( $\varepsilon$ )	$0.0721^{+0.0139}_{-0.0123}$	$0.034^{+0.004}_{-0.004}$	$0.070^{+0.015}_{-0.013}$	$0.007^{+0.001}_{-0.001}$
Kartvelishvili ( $\alpha$ )	$2.87^{+0.33}_{-0.35}$	$3.8^{+0.3}_{-0.3}$	$3.3^{+0.4}_{-0.4}$	$6.0^{+1.0}_{-0.8}$

Table 1: Extracted fragmentation function parameters.

The hemisphere observable used by H1 allows to investigate charm fragmentation also close to the kinematic threshold, by selecting events which do not contain a  $D^{*\pm}$  jet above the minimal  $E_T$  cut. The corresponding normalised  $D^{*\pm}$  meson cross sections together with the prediction of RAPGAP with the Kartvelishvili FF fitted to the data are shown in figure 5 d. The extracted fragmentation function is found to be significantly harder than the one fitted to the  $D^{*\pm}$  jet sample (the dotted line). This can be interpreted as an inadequacy of the QCD model to provide a consistent description of the full phase space down to the kinematic threshold. The NLO HVQDIS calculation fails to describe this data sample.

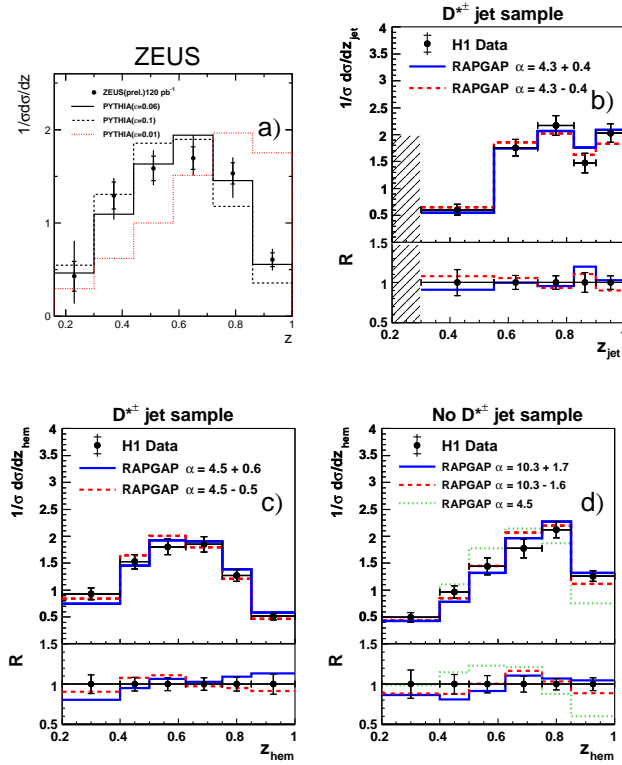


Fig. 5: Normalized  $D^{*\pm}$  meson cross sections as a function of the fragmentation observables: a)  $z_{jet}$  as measured by ZEUS, b)  $z_{jet}$  as measured by H1, c) and d)  $z_{hem}$  for the “ $D^{*\pm}$  jet” and the “no  $D^{*\pm}$  jet” samples. The full and dashed lines in the H1 sub-figures indicate a variation of  $\pm 1\sigma$  around the best fit value.



### 3 Beauty production at HERA

*Authors: S. Boutle, M. Turcato, A. Yagües-Molina*

#### 3.1 Introduction

At HERA, beauty quarks are produced predominantly via the boson-gluon fusion process, where a photon emitted by the electron interacts with a gluon in the proton producing a  $b\bar{b}$  pair. The measurements of such interactions are directly sensitive to the gluon density in the proton. Also, perturbative calculations of these processes should be reliable since the virtuality of the exchanged photon,  $Q^2$ , in the case of deep inelastic scattering (DIS), and the large mass of the produced quark, in the case of photoproduction, provide a hard scale. Hence, the study of  $b$  quark production at HERA is a stringent test of perturbative Quantum Chromodynamics (QCD). Measurements of such processes made at HERA are relevant for the LHC since they can test the precision of the description of  $b$  quark production by theoretical calculations. They also use tagging methods and event topologies which can be used to improve experimental techniques at the LHC. In the following, recent H1 and ZEUS measurements of beauty production are presented.

#### 3.2 Measurement of beauty photoproduction using semileptonic decays into leptons.

The installation of the silicon Micro-Vertex detector [20] (MVD) in the ZEUS detector [21] during the HERA luminosity upgrade period 2000/2001 allowed the heavy flavour measurements to reach higher precision. In one such measurement, beauty quarks were tagged by identifying a muon from the  $b$  semileptonic decay. The choice of a muon provides a clean experimental signature of the events. In this measurement two variables were used to discriminate between different quark decays. The first is the relative transverse momentum,  $p_T^{\text{rel}}$ , of the muon with respect to the heavy flavour hadron which for experimental purposes is approximated to the direction of the jet associated with the muon. This variable can be used to discriminate between beauty and charm decays since the mass of the beauty quark is larger, and therefore the  $p_T^{\text{rel}}$  spectrum for muons coming from  $b$  is harder. The second variable is the signed impact parameter,  $\delta$ , of the muon track. The absolute value of  $\delta$  is given by the transverse distance of closest approach of the track to the beam spot, where the beam spot position as a function of time is evaluated as the mean position of the event vertex over a proper event range. The sign of  $\delta$  is positive if the angle between the axis of the associated jet and the line joining the beam spot to the point of closest approach of the track is less than  $90^\circ$ , and is negative otherwise. The variable  $\delta$  reflects the lifetime of the quark and hence can be used to discriminate between charm and beauty decays and the decays of light quarks. The sign allows a statistical separation of detector resolution effects from the effects of the decay lifetime of the heavy hadron.

By fitting template distributions from Monte Carlo simulations of the  $p_T^{\text{rel}}$  and  $\delta$  variables to the data, the beauty fraction in the data can be extracted and used to calculate cross sections. The distributions of the  $p_T^{\text{rel}}$  and  $\delta$  variables are shown in Fig. 6 compared to MC predictions. The data are well described by the MC simulations.

The measurement presented here is based on a data sample collected during 2005 corresponding to an integrated luminosity of  $124 \text{ pb}^{-1}$ . Photoproduction ( $Q^2 < 1 \text{ GeV}^2$ ) events with  $0.2 < y < 0.8$ , having two jets with  $p_T^{j1,j2} > 7, 6 \text{ GeV}$ ,  $|\eta^{j1,j2}| < 2.5$  and a muon with  $p_T^\mu > 2.5$

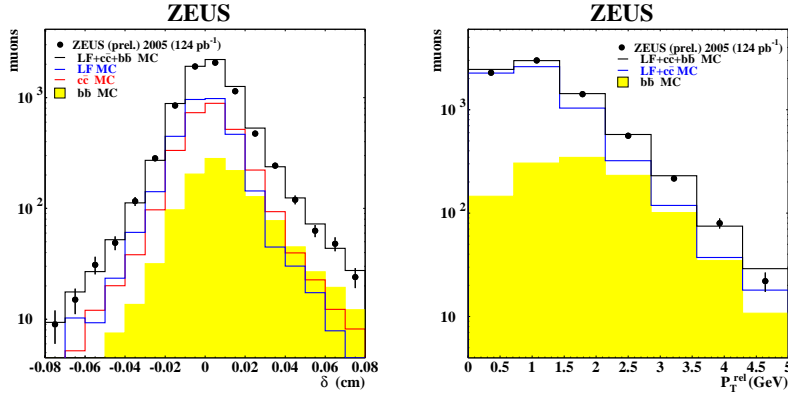


Fig. 6: Distribution of  $p_T^{\text{rel}}$  (left) and muon impact parameter  $\delta$  (right) of the data compared to the MC distributions for quarks of different flavour.

GeV and  $-1.6 < \eta^\mu < 2.3$  were selected. The event inelasticity,  $y$ , represents, in the proton rest frame, the fraction of the electron momentum which is transferred to the photon.

Figure 7 shows the distributions of the differential cross sections as a function of the muon transverse momentum,  $d\sigma/dp_T^\mu$ , and muon pseudorapidity  $d\sigma/d\eta^\mu$ . The results are compared to the ZEUS HERA-I data<sup>1</sup> [22] and to a NLO QCD prediction computed with the FMNR [14] program and corrected for hadronisation effects. The new results are in agreement with the previous measurement and compatible with NLO QCD predictions.

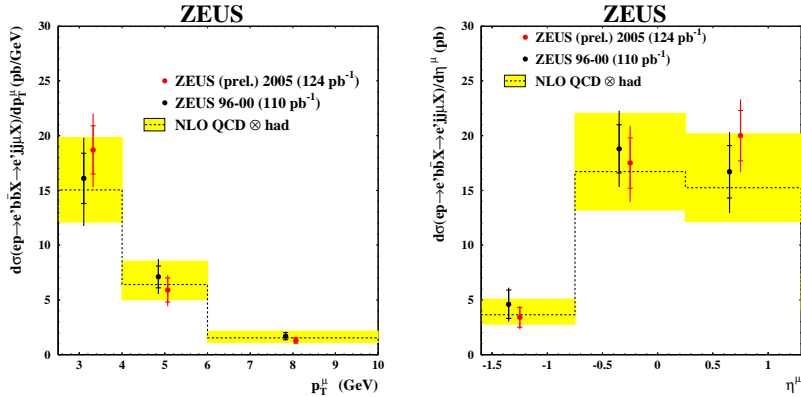


Fig. 7: Differential cross sections as a function of the muon transverse momentum,  $p_T^\mu$ , (left) and of the muon pseudorapidity,  $\eta^\mu$ , (right) for beauty photoproduction in dijet events with a muon. The measurements are compared to previous results and to NLO QCD predictions corrected for hadronisation effects.

Beauty photoproduction has been also measured using semileptonic decays to electrons or

<sup>1</sup>HERA-I refers to the data taken from 1996 to 2000 running period, previous to HERA luminosity upgrade.

positrons [23]. Tagging electrons has the advantage that lower values of the lepton transverse momentum are reachable. In this analysis, based on  $\mathcal{L} = 120 \text{ pb}^{-1}$  of HERA I data collected with the ZEUS detector from 1996 to 2000, events were selected in the photoproduction regime,  $Q^2 < 1 \text{ GeV}^2$ , having  $0.2 < y < 0.8$ , and with at least two jets with  $E_T^{j1,j2} > 7, 6 \text{ GeV}$ ,  $|\eta^{j1,j2}| < 2.5$  and an electron coming from the semileptonic  $b$  decay with  $p_T^e > 0.9 \text{ GeV}$  and  $|\eta^e| < 1.5$ . For the identification of the electrons and the extraction of the  $b$  fraction a likelihood ratio method was used combining five discriminating variables. Three of them were used mainly for the lepton identification, and are based on the ionisation energy loss of the particle in the ZEUS central drift chamber, and on other calorimeter and tracking information. The other two are the momentum of the electron candidate transverse to the jet direction,  $p_T^{\text{rel}}$ , and the azimuthal angle between the electron and the missing transverse momentum vector, which corresponds to the neutrino from the semileptonic  $b$  decay. Figure 8 shows the distributions of the differential cross sections as a function of the electron transverse momentum,  $d\sigma/dp_T^e$ , and pseudorapidity,  $d\sigma/d\eta^e$ . The data are compared with the predictions of the PYTHIA MC program, scaled by a factor 1.75, and with NLO QCD predictions from FMNR. The shape of the data is well described by both the MC and the NLO calculations. The NLO predictions describe the normalisation of the data within the large uncertainties.

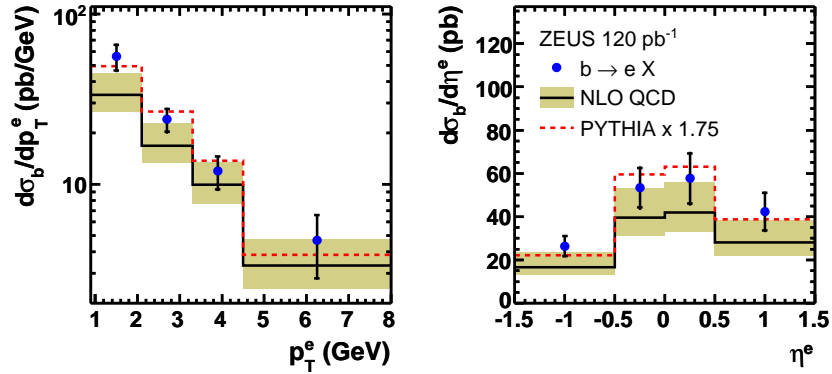


Fig. 8: Differential cross sections as a function of the transverse momentum,  $p_T^e$ , (left) and pseudorapidity,  $\eta^e$ , (right) of the electron for beauty photoproduction in dijet events with an electron. The measurements are compared to the predictions from PYTHIA as well as to NLO QCD calculations corrected for hadronisation effects.

### 3.3 Measurement of beauty dijet cross sections in photoproduction using inclusive lifetime tag.

An inclusive measurement of beauty in dijet events in the photoproduction regime [24] is presented here. The analysis is based on a sample of data collected by the H1 detector during the years 1999 and 2000 and corresponding to an integrated luminosity of  $56.8 \text{ pb}^{-1}$ . Photoproduction ( $Q^2 < 1 \text{ GeV}^2$ ) events with  $0.15 < y < 0.8$  and two jets with  $p_T^{j1,j2} > 11, 8 \text{ GeV}$  and  $-0.9 < \eta^{j1,j2} < 1.3$  were selected.

Events containing beauty quarks were distinguished from those containing only light quarks by reconstructing the signed impact parameter,  $\delta$ , of the charged tracks, i.e. their distances to the primary vertex, using precise spatial information from the H1 vertex detector. The long lifetime of  $b$  flavoured hadrons lead to larger displacements than for light quark events.

The quantities  $S_1$  and  $S_2$  are defined as the significance,  $\delta/\sigma(\delta)$ , of the track with the highest and second highest absolute significance, respectively, where  $\sigma(\delta)$  is the error on  $\delta$ . In order to reject most of the light quark background and to reduce the uncertainty due to the impact parameter resolution, the negative bins in the significance distributions were subtracted from the positive ones. To extract the beauty fraction, a simultaneous  $\chi^2$ -fit to the subtracted  $S_1$  and  $S_2$  distributions was performed (see Fig. 9). The differential cross sections as a function of  $p_T^j$  and  $\eta^j$ , shown in Fig. 10, are extracted using the scale factors obtained from the fit. The results are compared to different MC predictions and to NLO QCD calculations. The beauty cross sections are reasonably well described in shape, whereas the NLO QCD prediction seems to lie below the data.

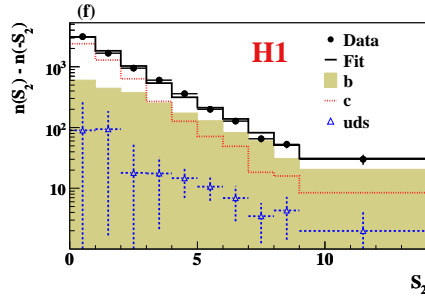


Fig. 9: Distributions of the subtracted signed significance for the sample with at least two tracks reconstructed in the Central Silicon Tracker.

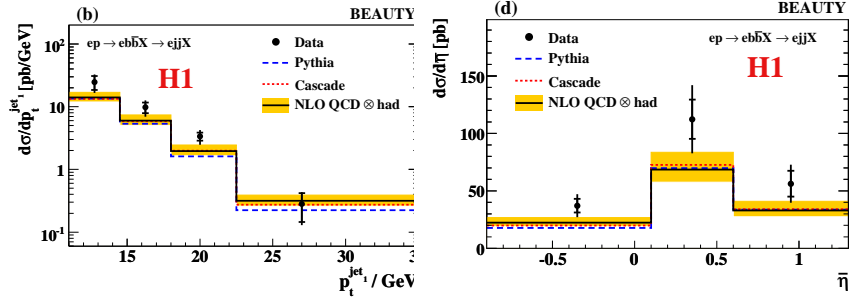


Fig. 10: Differential beauty dijet photoproduction cross sections as a function of the transverse momentum of the jet,  $d\sigma/dp_T^j$ , (left) and as a function of the jet pseudorapidity,  $d\sigma/d\eta^j$ , (right). The measurements are compared to the absolute predictions of PYTHIA and CASCADE as well as to NLO QCD calculations corrected for hadronisation effects.

### 3.4 Beauty production measurement using double tagging techniques

Beauty identification based on a single lepton tagging in dijet events is a powerful tool that allows to select a large event sample at HERA. However, the request of the presence of two jets in an event and the high background due to lighter flavour events does not allow the measurement of  $b$  quarks produced at very low transverse momenta, and therefore a total beauty cross section cannot be extracted. A way to access lower  $b$ -quark transverse momenta is to use double tagging techniques, by identifying two particles coming from the beauty decay. In this case, the cleaner event signature reduces significantly the background from non-beauty events.

An analysis [25] using this kind of approach identified beauty in events in which a  $D^*$  and a muon were found in the final state. Charm production is a background to this analysis, since a  $c\bar{c}$  pair in which one of the charm quarks hadronise into a  $D^*$  and the other produces a muon have a similar signature. However, in charm events the muon and the  $D^*$  lie in opposite hemispheres, while in the case of beauty production a muon and a  $D^*$  coming from the same  $B$  hadron lie in the same hemisphere, and in addition have opposite charges. Therefore, beauty and background can be separated by using the charge correlations and angular distributions of the muon with respect to the  $D^*$  meson.

The analysis uses a sample of  $\mathcal{L} = 114 \text{ pb}^{-1}$  of data corresponding to the full HERA I statistics collected by the ZEUS detector. The visible cross section was evaluated for unlike-sign  $D^*$ -muon events. This cross section was then extrapolated to the parton level and compared to NLO QCD predictions. No cut on the transverse momentum of the  $b$  quark,  $p_T^b$ , was imposed. The measured cross section in the kinematic region  $Q^2 < 1 \text{ GeV}^2$ ,  $\zeta^b < 1$ , where  $\zeta$  is the  $b$ -quark rapidity,  $0.05 < y < 0.85$  is

$$\sigma(ep \rightarrow b(\bar{b})X) = 11.9 \pm 2.9(\text{stat.})_{-3.3}^{+1.8}(\text{syst.}) \text{ nb}, \quad (1)$$

to be compared to a NLO QCD prediction of

$$\sigma^{NLO}(ep \rightarrow b(\bar{b})X) = 5.8_{-1.3}^{+2.1} \text{ nb}. \quad (2)$$

The measured cross section exceeds the NLO QCD prediction, but is compatible within the errors.

In another double-tagging analysis [26], events with two muons in the final state were used to study beauty production. This method has many advantages over the the  $D^*\mu$  analysis. It has larger statistics due to the higher branching ratio; the kinematic region is larger allowing the extraction of the total beauty cross section with almost no extrapolation; lower background induced by charm allows  $b\bar{b}$  correlations to be measured, testing the contribution of higher orders in perturbative calculations. The analysis uses  $114 \text{ pb}^{-1}$  of HERA I data collected by the ZEUS detector. The data sample is separated into high- and low-mass (isolated and non-isolated), like- and unlike-sign muon pairs. Since beauty is the only genuine source of like-sign muon pairs and fake muon background can give rise to like- and unlike-sign pairs, the beauty contribution can be determined from the difference between the like- and unlike-sign samples.

The kinematic region for the measurement of the total cross section was kept as large as possible:  $-2.2 < \eta^\mu < 2.5$ ,  $p_T^\mu > 1.5 \text{ GeV}$  for one muon and  $p_T^\mu > 0.75 \text{ GeV}$  for the other muon, as well as  $p > 1.8 \text{ GeV}$  for  $\eta < 0.6$ , or ( $p > 2.5 \text{ GeV}$  or  $p_T > 1.5 \text{ GeV}$ ) for  $\eta > 0.6$ .

Also in this case, a visible cross section was measured and then extrapolated to the total beauty cross section. DIS and photoproduction regimes were not separated. The measured total beauty cross section is

$$\sigma_{\text{tot}}(ep \rightarrow b\bar{b}X) = 13.9 \pm 1.5(\text{stat.})_{-4.3}^{+4.0}(\text{syst.}) \text{ nb.} \quad (3)$$

The NLO QCD prediction was obtained by adding the predictions from FMNR and HVQDIS [27] for the photoproduction and DIS parts, respectively:

$$\sigma_{\text{tot}}^{\text{NLO}}(ep \rightarrow b(\bar{b})X) = 7.5_{-2.1}^{+4.5} \text{ nb.} \quad (4)$$

Also in this case, the NLO QCD prediction is lower than the measured value, but compatible within the large uncertainties.

Visible differential cross sections were also measured, in the kinematic region defined by  $p_T^\mu > 1.5 \text{ GeV}$ ,  $-2.2 < \eta^\mu < 2.5$  for both the muons, in order to ensure a uniform kinematic acceptance. Figure 11 shows the the differential cross sections as a function of the muon transverse momentum,  $d\sigma/dp_T^\mu$ , and pseudorapidity,  $d\sigma/d\eta^\mu$ . The data are well described in shape by the theoretical predictions, with a tendency of the NLO QCD calculations to underestimate the normalisation of the data consistent with the observations from the total cross section.

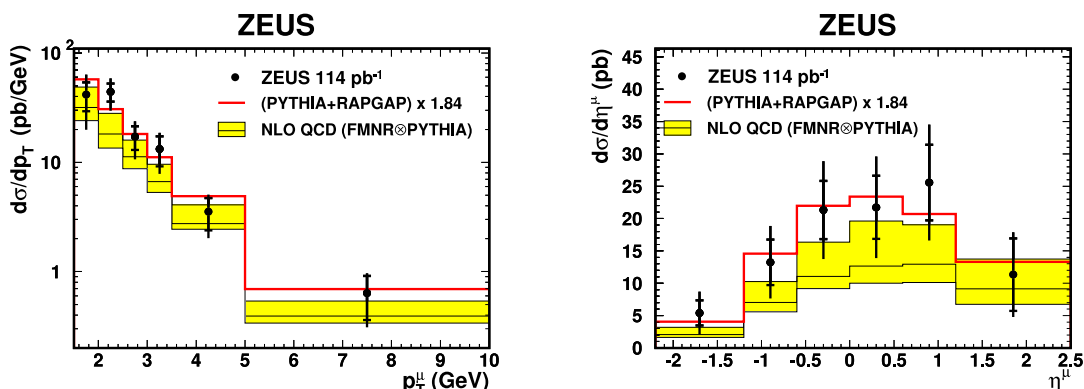


Fig. 11: Differential cross sections  $d\sigma/dp_T^\mu$  (left) and  $d\sigma/d\eta^\mu$  (right) for muons from  $b$  decays in dimuon events. The measurements (solid dots) are compared to the scaled sum of the predictions by the LO+PS generators PYTHIA and RAPGAP (histogram) and to the NLO QCD predictions from FMNR  $\otimes$  PYTHIA.

### 3.5 Conclusions

Beauty production at HERA is extensively studied using different analysis techniques. Beauty tagging with a single lepton gives a high statistics sample for the analyses, and the precision of the measurements is now comparable or better than that of the theoretical predictions. The measurements based on electron and muon tagging are affected by different systematic uncertainties, cover a slightly different kinematic region, and cross check each other. Inclusive analyses based on lifetime are also being done and will reach their full potential when the full HERAII data sample will be used. This kind of analyses are sensitive to beauty production also at large  $p_T^b$ .

For the investigation of the lower  $p_T^b$  region, double tagging techniques have been developed. In this way, the total beauty production cross section can be measured. Although these

measurements are still affected by a relatively large statistical uncertainty, they show that the difference between the observed cross sections and the theoretical predictions is not larger at lower transverse momenta.

The study of beauty production at HERA is significantly testing the precision of the perturbative QCD predictions, over a wide range in  $p_T$  and  $\eta$  of the produced  $b$  quarks. The understanding of beauty production in terms of perturbative QCD is vital for the future measurements that will be done at the large hadron collider, where a significant part of the cross section will consist on beauty.

## 4 Experimental Status of $F_2^{c\bar{c}}$ and $F_2^{b\bar{b}}$ at HERA

Authors: Philipp Roloff, Monica Turcato

### 4.1 Theoretical description

The double differential cross section versus  $x$  and  $Q^2$  for the production of a heavy quark (charm or beauty) pair,  $Q\bar{Q}$ , in deep inelastic scattering can be described by the heavy quark contributions to the proton structure functions:

$$\frac{d^2\sigma^{Q\bar{Q}}(x, Q^2)}{dx dQ^2} = \frac{2\pi\alpha^2}{Q^4 x} \left\{ [1 + (1-y)^2] F^{Q\bar{Q}}(x, Q^2) - y^2 F_L^{Q\bar{Q}}(x, Q^2) \right\}. \quad (5)$$

In the simplified picture of the quark-parton model (QPM) the electron scatters off a single quark in the proton. In this case  $x$  can be interpreted as the fraction of the proton momentum carried by the struck quark. Since heavy quarks can not exist within the proton due to their high mass, they are dominantly produced by the boson gluon fusion (BGF) process.

Heavy quark production as described above can be interpreted in two ways: on one hand it is possible to treat charm and beauty as massive quarks which are produced dynamically in the scattering process. In this case  $F_2^{c\bar{c}}$  and  $F_2^{b\bar{b}}$  provide an indirect measurement of the gluon content of the proton. On the other hand it is possible to consider the splitting of a gluon into a heavy quark pair to happen within the proton for  $Q^2 \gg (2m_Q)^2$ . Hence here  $F_2^{c\bar{c}}$  and  $F_2^{b\bar{b}}$  give the virtual charm and beauty content of the proton. As a consequence, the use of i.e.  $Z$  boson production as a luminosity monitor at the LHC requires a precise knowledge of the beauty content of the proton.

The large masses ( $m_c, m_b \gg \Lambda_{QCD}$ ) of the charm and beauty quarks provide an additional hard scale in perturbative QCD calculations. Different approaches exist to describe the multi scale problem of heavy quark production in  $ep$  collisions. In the massive or fixed flavour number scheme (FFNS) the proton contains only light quarks while charm and beauty are produced dynamically. Thus the threshold region is handled correctly, but the presence of other large scales, e.g.  $Q^2$  or the transverse momentum of the heavy quarks,  $p_T$ , can spoil the convergence of the perturbative expansion. In contrast, charm and beauty are treated as massless partons within the proton in the zero mass variable flavour number scheme (ZM-VFNS) which can improve the reliability of the calculations if one of the competing scales becomes large. An interpolation between both approaches is done in the (general mass) variable flavour number scheme (GM-VFNS) where heavy flavour production is treated as massive at low  $Q^2$  and massless at high  $Q^2$ .

While precise measurements of charm production are feasible using the large HERA II data sample, the measurements of beauty production are usually limited by the small production cross section. Since effects due to the higher beauty mass are relevant in a large part of the phase space accessible at HERA, beauty production might help to improve the understanding of mass effects for heavy quark production in deep inelastic scattering. A possible scenario is to “calibrate” theory predictions using beauty production and apply the improvements to charm for the extraction of the gluon content of the proton.



## 4.2 Experimental results on $F_2^{c\bar{c}}$

The charm contribution to the proton structure function  $F_2$ ,  $F_2^{c\bar{c}}$ , has been measured at HERA by the two Collaborations ZEUS [28–31] and H1 [32–35], in a wide kinematic region in  $x$  ( $0.00002 \lesssim x \lesssim 0.03$ ) and in the photon virtuality,  $Q^2$  ( $1 < Q^2 < 1000 \text{ GeV}^2$ ).

Charm production at HERA can be tagged in different ways. In the so-called *golden mode* a  $D^*(2010)$  meson is reconstructed through its decay  $D^{*+} \rightarrow D^0\pi^+ \rightarrow K^-\pi^+\pi^+$  (+c.c.). Other charmed mesons can also be reconstructed: the most copiously produced are  $D^0$ ,  $D^\pm$ ,  $D_s$ . The production cross sections of all these mesons can be measured in a defined kinematic region, and the total charm cross section can then be extracted by extrapolating the measurements to the full phase space. This extrapolated cross section is then used to evaluate  $F_2^{c\bar{c}}$ . Both the ZEUS and the H1 Collaborations have used this method to extract  $F_2^{c\bar{c}}$  from  $D$  mesons cross sections. Charm tagging with mesons gives a clean signature of charm production, but the extrapolation to the total charm cross section can be large, especially in the low  $Q^2$  region (as an example, at ZEUS typical extrapolation factors range from  $\sim 4$  in the low- $Q^2$ , low- $x$  region to 1.5 at high- $Q^2$  [28]).

An alternative method to tag charm production takes advantage of the long lifetime of the charmed particles, by reconstructing secondary vertices from  $D$ -meson decay products, or, in inclusive analyses, by identifying tracks having impact parameter,  $\delta$ , significantly displaced from the event vertex. The secondary vertex reconstruction for  $D^\pm$  and  $D^0$  mesons has been used by the ZEUS Collaboration to enhance the signal to background ratio, and therefore the statistical precision, of the measurement [31]. On the other side, fully inclusive analyses use the significance of the impact parameter of the highest impact parameter tracks to separate charm and beauty from light flavour production [33, 34], since heavy flavours show a longer tail in the positive side of this distribution. The fraction of charm and beauty in an inclusive data sample can therefore be extracted by fitting the significance distribution to the contributions from beauty, charm, and lighter quarks. This method has been used by the H1 Collaboration to obtain some of the results presented here [33–35].

The advantage of the inclusive method is that the kinematic region for the measurement of charm production is significantly enlarged, and therefore the extrapolation needed for the measurement of  $F_2^{c\bar{c}}$  is strongly reduced.

The program HVQDIS [27] is the only program which is able to provide theoretical predictions for  $D$  meson production cross sections at NLO accuracy in perturbative QCD. It was used by the ZEUS and H1 Collaborations to extrapolate the measured cross section for a particular  $D$  meson final state to  $F_2^{c\bar{c}}$ . In this program, the production of heavy flavours is performed using the fixed flavour number scheme. The ZEUS and H1 measurements of  $F_2^{c\bar{c}}$  extracted in this way should therefore be compared with NLO QCD predictions evaluated in the FFNS.

The results for  $F_2^{c\bar{c}}(x, Q^2)$  are shown in Fig. 12. In the figure the ZEUS and H1 measurements, obtained from charmed meson production, are compared with the H1 results from inclusive lifetime measurements. The agreement between the experiments is good, validating the two different analysis procedures. The data rise with increasing  $Q^2$ , with the rise becoming steeper at lower  $x$ .

The data are also compared with perturbative QCD predictions at NLO. Two different parameterisations of the proton PDFs have been used for the NLO QCD calculations, in or-

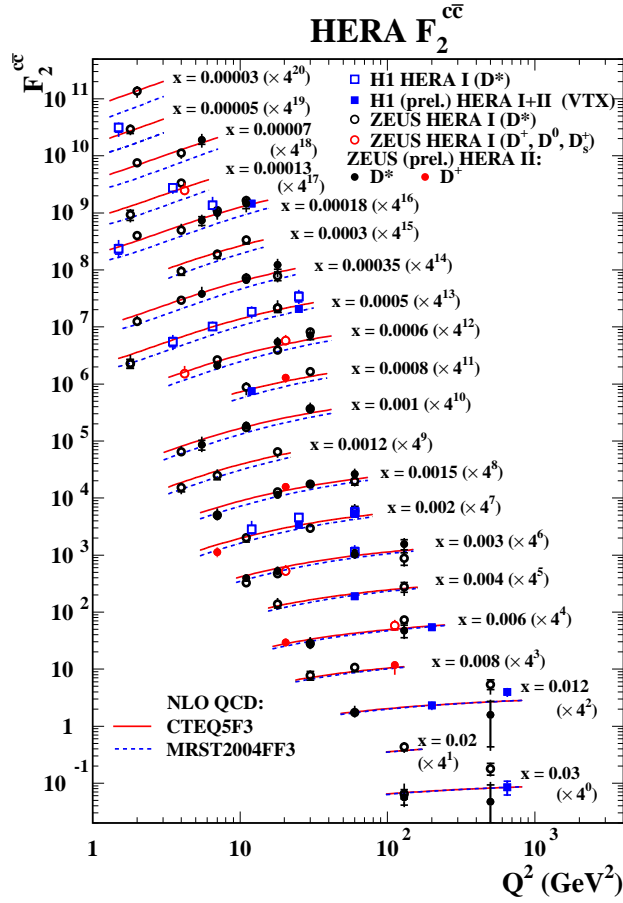


Fig. 12: The measured  $F_2^{c\bar{c}}$  at  $x$  values between 0.00003 and 0.03 as a function of  $Q^2$ . The data are shown with statistical uncertainties (inner bars) and statistical and systematic uncertainties added in quadrature (outer bars). The data are compared with next-to-leading order QCD predictions, evaluated using different proton PDFs.

der to check the sensitivity of the predictions to different gluon densities: CTEQ5F3 [36] and MRST2004FF3 [37]. The charm data are in general well described by NLO QCD: this shows that the proton PDFs, which are extracted mainly from inclusive scattering data, are also able to describe reasonably well charm production. The two PDFs show differences in the low  $x$  region, demonstrating the sensitivity of the measurement to different parameterisation of the gluon density in the proton.

### 4.3 Experimental results on $F_2^{b\bar{b}}$

The beauty contribution to the inclusive structure function  $F_2$  was measured by the ZEUS Collaboration using muons and jets and by the H1 Collaboration from lifetime information of displaced tracks.

The ZEUS Collaboration measured beauty production in events with a muon and a jet,

using a data sample of  $\mathcal{L} = 39 \text{ pb}^{-1}$ . The fraction of beauty quarks in the data was derived using the distribution of the transverse momentum of the muon relative to the axis of the associated jet,  $p_T^{\text{rel}}$  [38]. Due to the larger mass of the beauty quark, muons originating from  $b$  decays tend to higher values of  $p_T^{\text{rel}}$  compared to muons from charm and light flavour decays. The beauty contribution to  $F_2$ ,  $F_2^{b\bar{b}}$ , was obtained by extrapolating the double differential cross sections as a function of  $Q^2$  and  $x$  to the full phase space using the HVQDIS program, as for the extraction of  $F_2^{c\bar{c}}$  from the visible cross sections for  $D$  meson production. Here extrapolation factors between 3 and 6 decreasing with  $Q^2$  had to be applied.

The H1 collaboration extracted  $F_2^{b\bar{b}}$  in a fully inclusive analysis based on information from the Central Silicon Tracker. The impact parameter significance of tracks in the transverse plane was used in a fit to extract the (charm and) beauty fractions in the considered data sample [35]. Due to the long lifetime of the  $B$  hadrons, it is possible to distinguish the position of the decay vertices of these particles from the primary interaction vertex. As a consequence, tracks originating from beauty decays exhibit large positive impact parameters compared to tracks coming from lighter quarks. An advantage of the inclusive lifetime method is that the extrapolation to the full phase space is smaller. Recent results from the HERA II period were combined with earlier measurements [33, 34].

The results obtained by the H1 and ZEUS Collaborations are summarised in Fig. 13. The reduced cross section

$$\tilde{\sigma}^{b\bar{b}} = F_2^{b\bar{b}} - \frac{y^2}{1 + (1 - y)^2} F_L^{b\bar{b}}, \quad (6)$$

is shown as a function of  $x$  for different values of  $Q^2$ . Although very different methods have been used, the results are in agreement within the large errors.

The data are compared to NLO QCD predictions using different schemes [39]. The CTEQ5F4 [36] is done in the FFNS, while MRST04 [40], MRST NNLO [41] and CTEQ6.5 [42] implement the VFNS. At low values of  $Q^2$  and  $x$  the predictions of the CTEQ and MRST groups differ up by a factor two, but the present statistical accuracy of the data does not allow to discriminate between the different calculations. A better precision of the data is needed in order to better understand the different aspects of the theoretical calculations and to disentangle between different approaches.

#### 4.4 Conclusions and outlook

Both experiments, H1 and ZEUS, collected a data sample of about  $0.5 \text{ fb}^{-1}$ . The analysis of the full HERA I+II dataset will increase the available statistics by a factor of 2 to 10, depending on the analysis. The combination of different heavy flavour tagging methods (e.g. different  $D$  mesons for charm, different leptons for beauty, inclusive analyses) can further improve the precision of the measurements, keeping also into account the fact that the systematic uncertainties of different tagging techniques are at least partially uncorrelated. The final step is the combination of the ZEUS and H1 data into a single measurement: this will again double the available dataset.

New detector components, which allow to extend the kinematic range of the  $F_2^{c\bar{c}}$  and  $F_2^{b\bar{b}}$  measurements, were installed for the HERA II data taking period. The forward region can be studied using the ZEUS Straw Tube Tracker and Forward Microvertex Detector while the H1

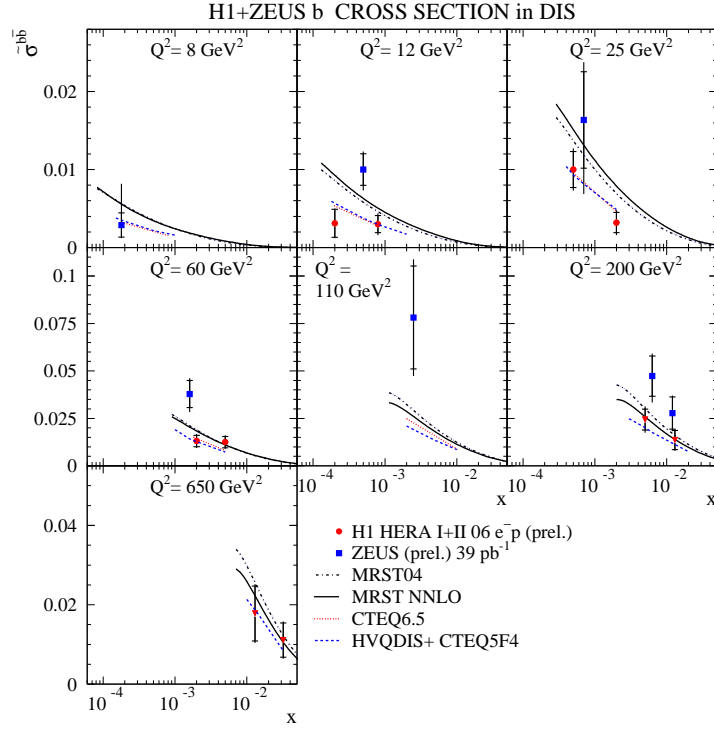


Fig. 13:  $\hat{\sigma}^{b\bar{b}}$  as a function of  $x$  for different values of  $Q^2$ . The inner error bars represent the statistical uncertainties only while the outer error bars correspond to statistical and systematic uncertainties added in quadrature. Different predictions are compared to the data.

Backward Silicon Tracker gives access to the backward region.

Significant improvement in the precision of the measurements is therefore possible and will be reached by the final HERA analyses. The new beauty measurements will be of help to understand some aspects of the theory that will be then implemented for the description of charm production. A final combined ZEUS+H1 measurement of charm production could be used in the PDF fits and will hopefully help to learn something more on the gluon density in the proton.

## References

- [1] H1 Collaboration, H1prelim-08-072, [https://www-h1.desy.de/publications/H1preliminary.short\\_list.html#HQ](https://www-h1.desy.de/publications/H1preliminary.short_list.html#HQ), 2008.
- [2] H1 Collaboration, A. Aktas *et al.*, Eur. Phys. J. C **51**, 271 (2007).
- [3] H1 Collaboration, H1prelim-08-073, [https://www-h1.desy.de/publications/H1preliminary.short\\_list.html#HQ](https://www-h1.desy.de/publications/H1preliminary.short_list.html#HQ) (2008).
- [4] H1 Collaboration, A. Aktas *et al.*, arXiv 0808.1003 (hep-ex) 2008.

- [5] ZEUS Collaboration, ZEUS-prel-07-008,  
[http://www-zeus.desy.de/physics/hfla/public/abstracts07/paper/f2charm\\_zeus\\_EPSPaper\\_106.ps](http://www-zeus.desy.de/physics/hfla/public/abstracts07/paper/f2charm_zeus_EPSPaper_106.ps), 2008.
- [6] ZEUS Collaboration, S. Chekanov et al., Phys. Lett. **B649**, 111-121 (2007).
- [7] ZEUS Collaboration, S. Chekanov et al., DESY-08-129, arXiv:0807.1290 [hep-ex] (2008).
- [8] ZEUS Collaboration, S. Chekanov et al., JHEP **0707**, 74 (2007).
- [9] ZEUS Collaboration, ZEUS-prel-07-010,  
<http://www-zeus.desy.de/physics/hfla/public/abstracts07/>, 2008.
- [10] A. Baird et al., IEEE Trans. Nucl. Sci. **48**, 1276 (2001).
- [11] A. Schöning, Nucl. Instr. and Meth. **A518**, 542 (2004).
- [12] A.W. Jung et al., *First Results from the Third Level of the H1 Fast Track Trigger*, Proc. of the 2007 IEEE NPSS RealTime Conference, Chicago, USA, 2007.
- [13] H1 Collaboration, A. Aktas *et al.*, Eur. Phys. J. **C 50**, 251 (2006).
- [14] S. Frixione, M.L. Mangano, P. Nason and G. Ridolfi, Phys. Lett. **B 348**, 633 (1995).
- [15] U. Bassler, G. Bernardi, Nucl. Instr. and Meth. **A361**, 197 (1995).
- [16] H. Jung, PDF4MC, <http://indico.cern.ch/conferenceDisplay.py?confId=36364>, 2008.
- [17] H1 Collaboration, A Aktas *et al.*, *Study of Charm Fragmentation into  $D^{*\pm}$  Mesons in Deep-Inelastic Scattering at HERA*, [arXiv:0808.1003], submitted to Eur. Phys. J. **C**
- [18] S. Fang [ZEUS Collaboration], “Charm fragmentation function and charm fragmentation fractions at ZEUS,” Proceedings DIS 2007, Munich, Germany, April 16 – 20, Eds. G. Grindhammer and K. Sachs, 10.3360/dis.2007.147
- [19] ALEPH Collaboration, S. Schael *et al.*, Phys. Lett. **B 606**, 265 (2005); G. Rudolph [ALEPH collaboration], private communication.
- [20] E.N. Koffeman *et al.*, Nucl. Instrum. Meth. **A 453**, 89 (2000).  
D. Dannheim *et al.*, Nucl. Instrum. Meth. **A 505**, 663 (2003).
- [21] ZEUS Collaboration, U. Holm(ed.), *The ZEUS Detector*. Status Report (Unpublished), DESY (1993), available on  
<http://www-zeus.desy.de/bluebook/bluebook.html>
- [22] ZEUS Collaboration, S. Chekanov *et al.*, Phys. Rev. **D 70**, 012008 (2004).
- [23] ZEUS Collaboration, S. Chekanov *et al.*, DESY-08-056 (May 2008).
- [24] H1 Collaboration, A. Aktas *et al.*, Eur. Phys. J. **C47**, 597-610 (2006).

- [25] ZEUS Collaboration, S. Chekanov *et al.*, Eur. Phys. J. **C50** 299-314 (2007).
- [26] ZEUS Collaboration, S. Chekanov *et al.*, DESY-08-129 (2008).
- [27] B.W. Harris and J. Smith, Phys. Rev. **D 57**, 2806 (1998).
- [28] ZEUS Collaboration, S. Chekanov *et al.*, Phys. Rev. **D 69**, 012004 (2004).
- [29] ZEUS Collaboration, S. Chekanov *et al.*, JHEP **07**, 074 (2007).
- [30] M. Turcato [ZEUS Collaboration], Proc. of the 2007 Europhysics Conference on High Energy Physics, Manchester, England, July 2007, [http://www.iop.org/EJ/article/1742-6596/110/2/022054/jpconf8\\_110\\_022054.pdf](http://www.iop.org/EJ/article/1742-6596/110/2/022054/jpconf8_110_022054.pdf)
- [31] D. Nicholass [ZEUS Collaboration], Proc. of 15th Int. Workshop on Deep-Inelastic Scattering and Related Subjects, Munich, April 2007, <http://dx.doi.org/10.3360/dis.2007.145>
- [32] H1 Collaboration, A. Aktas *et al.*, Phys. Lett. **B 528**, 199 (2002).
- [33] H1 Collaboration, A. Aktas *et al.*, Eur. Phys. J. **C 45**, 23 (2006).
- [34] H1 Collaboration, A. Aktas *et al.*, Eur. Phys. J. **C 40**, 349 (2005).
- [35] H1 Collaboration, *Submitted to the 23rd International Symposium on Lepton-Proton Interactions at High Energy, LP2007*, Daegu, Republic of Korea, August 13-18, 2007.
- [36] CTEQ Collaboration, Eur. Phys. J. **C 12**, 375 (2000).
- [37] A. D. Martin, W. J. Stirling and R. S. Thorne, Phys. Lett. **B 636**, 259 (2006).
- [38] B. Kahle [ZEUS Collaboration], Proc. of 15th Int. Workshop on Deep-Inelastic Scattering and Related Subjects, Munich, April 2007, <http://dx.doi.org/10.3360/dis.2007.164>
- [39] P.D. Thompson, arXiv:hep-ph/0703103v1, 2007.
- [40] A.D. Martin *et al.*, Eur. Phys. J. **D 73**, 050419 (2006).
- [41] R.S. Thorne, Phys. Rev. D **73**, 050419 (2006).
- [42] W.K. Tung *et al.*, JHEP **02**, 259 (2006).